The K_v channel blocker 4-aminopyridine enhances Ag^+ uptake: A scanning electrochemical microscopy study of single living cells

Dongping Zhan, Fu-Ren F. Fan, and Allen. J. Bard*

Department of Chemistry and Biochemistry, University of Texas, 1 University Station A5300, Austin, TX 78712-0165

Contributed by Allen J. Bard, June 2, 2008 (sent for review March 5, 2008)

We report that silver ion (Ag^+) uptake is enhanced by 4-aminopyridine (4-AP), a well known voltage-sensitive potassium ion channel (K_v) blocker. Both bacterial (*Escherichia coli*) and mammalian (3T3 fibroblast) cells were used as model systems. Ag^+ uptake was monitored with a scanning electrochemical microscope with an amperometric Ag^+ ion-selective electrode (Ag^+-ISE) and the respiration rates of *E. coli* cells were measured by oxygen reduction at an ultramicroelectrode. The results showed that not only the amount but also the rate of silver uptake by the cells increased significantly when 4-AP was added to the solution. For fibroblasts, the Ag^+ uptake rate was 4.8×10^7 ions per cell per sec without 4-AP compared with 1.0×10^8 ions per cell per sec with 0.2 mM 4-AP. For *E. coli* cells, the uptake rate was 1.5×10^4 ions per cell per sec without 4-AP vs. 3.5×10^4 ions per cell per sec with 0.5 mM 4-AP and 5.9×10^4 ions per cell per sec with 1 mM 4-AP. Thus, 4-AP might be useful where silver is used as antimicrobial agent to speed its uptake.

E. coli | scanning electrochemical microscope | silver ion

Ag^+ has been used as an antimicrobial drug for centuries (1, 2). The antimicrobial activity of Ag^+ involves the complex reaction with membranes, enzymes, nucleic acids, and other cellular components. As a soft acid, Ag^+ interacts with electron donor groups containing nitrogen, oxygen, and sulfur that are present in microbial cells as amines, hydroxide groups, phosphates, and thiols. Thiol group-containing enzymes, such as lactate dehydrogenase, are proposed to be inhibited after binding of Ag^+ (3, 4). Ag^+ has also been shown to affect the respiratory chain (5–7). Other potential sites of action for Ag^+ are associated with energy-yielding reactions of the respiratory chain, collapse of proton motive force, and interference with phosphate uptake (8, 9). Ag^+ may also compete for cellular entry in an essential copper transport system (10, 11). Ag^+ accumulation may occur in two stages: a rapid, reversible, and metabolically independent surface binding followed by metabolically dependent, irreversible intercellular accumulation (12, 13). Silver toxicity has also been studied in mammalian cells such as fibroblasts and keratinocyte cells (14, 15).

The current antimicrobial use of silver has promoted concerns over silver resistance. Silver-resistant bacterial strains have been isolated from both clinical and environmental sources (16, 17). In Gram-negative bacteria, at least two general mechanisms effectively reduce Ag^+ access: the outer membrane porins and active efflux systems (18, 19). Most toxic heavy metal resistances result not from chemical detoxification, but from energy-dependent ion efflux from the cell via channels that function either as ATPases or as chemiosmotic cation/proton antiporters. The molecular genetics of a silver efflux pump has been described; the gene cluster for silver resistance contains a total of nine genes, seven of which have been named and two less-recognized ORFs that are still called ORFs: *silP ORF105 silA silB ORF96 silC silS silR silE* (20). The steady state between the uptake, absorption, and efflux processes determines the Ag^+ efficacy.

Although Ag^+ toxicity and resistance have been investigated extensively, to our knowledge, the mechanism of silver uptake remains uncertain. Here, we suggest a relationship between Ag^+ uptake and K_v channels through a study of the effect of 4-aminopyridine (4-AP), a well known broad-spectrum blocker of K_v channels (21, 22). The action of 4-AP on K_v channels is complicated and depends on many factors as has been discussed in detail (21–24). 4-AP can penetrate the cell membrane, act on the cytoplasmic side of K_v channels, block the K_v channels from assuming their "on" (K^+ passing) state, and become trapped in the channel once it is closed or inactivated. In general, the K_v channels with greater 4-AP sensitivity have a slower "off" rate. We show that 4-AP increases the rate of Ag^+ uptake and this suggests involvement of the K_v channels.

The scanning electrochemical microscope (SECM) has become a useful tool for exploring bioprocesses occurring on single living cells, because SECM can provide a spatial image of electrochemical (EC) reactivity as well as cell topography (25–27). Our group reported investigations on the action of multidrug resistance (MDR) pumps on menadione in human Hep G2 and yeast cells (28, 29). In this article, we used an amperometric Ag^+ ion-selective electrode (Ag^+-ISE) to monitor the Ag^+ uptake by *Escherichia coli* and fibroblasts in real time (30). The cell viability for different Ag^+ treatments was characterized by studying cell respiration by SECM. The results showed that Ag^+ uptake by *E. coli* and fibroblasts are enhanced significantly when 4-AP is present, suggesting involvement of the K_v channel. Cell proliferation was inhibited and the toxic effect of Ag^+ was promoted, causing loss of cell viability. This suggests possible applications in Ag^+-based therapeutics and conceivably applications in bioremediation for environmental purposes (31).

Results

Electrochemical Detection with the Micropipet Supported Ag^+-ISE. The electrochemistry of the interface between two immiscible electrolyte solutions (ITIES) provides a sensitive voltammetric method to detect the ion concentration in aqueous solution (32, 33). Recently, we developed an Ag^+-ISE tip supported by a micrometer-sized micropipet as an SECM tip to determine the Ag^+ concentration in the vicinity of single living cells (30). The internal solution was 5 mM silver ionophore IV and 5 mM bis(triphenylphosphoranylidene)ammonium tetrakis(4-chlorophenyl)borate (BTPPATPBCl) dissolved in 1,2-dichloroethane (DCE). The solution was injected into a micropipet, which was then inserted into a sulfate medium. Because DCE is immiscible with the aqueous sulfate medium, an ITIES was formed at the tip of the micropipet. A silver tetrakis(4-chlorophenyl)borate

Author contributions: D.Z., F.-R.F.F., and A.J.B. designed research; D.Z. and F.-R.F.F. performed research; D.Z., F.-R.F.F., and A.J.B. analyzed data; and D.Z., F.-R.F.F., and A.J.B. wrote the paper.

The authors declare no conflict of interest.

*To whom correspondence should be addressed. E-mail: ajbard@mail.utexas.edu.

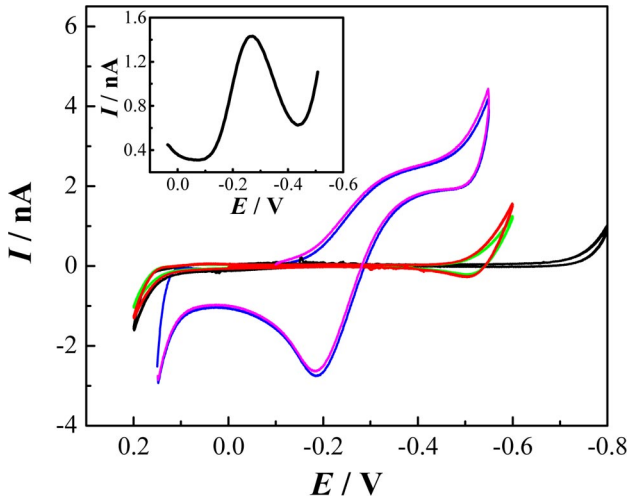

Fig. 1. Cyclic voltammograms of the potential windows and facilitated Ag^+ ion transfer by silver ionophore IV (L) at a scanning rate of 50 mV/s: (*i*) black line, Ag|AgTPBCl|5 mM L + 5 mM BTPPATPBCl (DCE)‖75 mM Na_2SO_4 (W)|polypyrrole|steel; (*ii*) red line, Ag|AgTPBCl|5 mM L + 5 mM BTPPATPBCl (DCE)‖75 mM Na_2SO_4, 1 mM $MgSO_4$ + 3 mM K_2SO_4 (W)|polypyrrole|steel; (*iii*) green line, Ag|AgTPBCl|5 mM L + 5 mM BTPPATPBCl (DCE)‖75 mM Na_2SO_4, 1 mM $MgSO_4$ + 3 mM K_2SO_4 + 0.5 mM 4-AP (W)|polypyrrole|steel; (*iv*) blue line, Ag|AgTPBCl|5 mM L + 5 mM BTPPATPBCl (DCE)‖75 mM Na_2SO_4, 1 mM $MgSO_4$ + 3 mM K_2SO_4 + 0.1 mM Ag_2SO_4 (W)|polypyrrole|steel; (*v*) magenta line, Ag|AgTPBCl|5 mM L + 5 mM BTPPATPBCl (DCE)‖75 mM Na_2SO_4, 1 mM $MgSO_4$ + 3 mM K_2SO_4 + 0.5 mM 4-AP + 0.1 mM Ag_2SO_4 (W)|polypyrrole|steel. The insert is a differential pulse voltammogram of case 5, the sweep rate is 20 mV/s, the pulse amplitude is 50 mV, the sample width is 20 ms, the pulse width is 50 ms, and the pulse period is 200 ms.

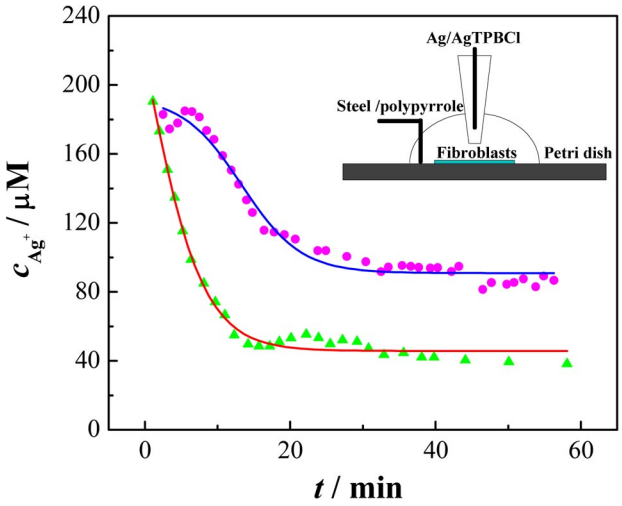

Fig. 2. Ag^+ concentration changes with time when fibroblasts exposed to (*i*) 0.1 mM Ag_2SO_4 (magenta circle) and (*ii*) 0.1 mM Ag_2SO_4 and 0.2 mM 4-AP (green triangle). (*Inset*) Schematic diagram for detection of Ag^+ concentration in the bulk drop.

(AgTPBCl)-coated silver wire was inserted into the micropipet, and a polypyrrole-coated stainless steel wire was inserted into the aqueous sulfate medium. When an appropriate potential was applied across the DCE/water interface, silver ion transferred across it, from the aqueous to the DCE phase, facilitated by the silver ionophore. As a result, a current was obtained that represented the flux of Ag^+. Our previous study showed that the relationship between the cyclic voltammetric (CV) peak or limiting current and the Ag^+ concentration was linear and gave a detection limit down to 0.1 μM. Curve 4 in Fig. 1 shows typical CV scans of the facilitated Ag^+ transfer. The asymmetric voltammogram is caused by the asymmetric diffusion field inward/outward at the micropipet tip, as described in ref. 30. Curves 1–3 show the potential windows in different cases without Ag^+ in the aqueous solution. The potential window in the absence of Ag^+ is limited by the presence of K^+ ion, which is easier to transfer across the DCE/water interface than Na^+ and Mg^{2+}. The potential window did not change with the presence of 4-AP (shown as curve 5), which exists in aqueous solution as a cation at a pH of 6.5, indicating that the 4-AP cation is more difficult to transfer across the DCE/water interface than K^+ ion. When silver ionophore IV was present in DCE phase, as shown in curves 4 and 5, the 4-AP cation did not interfere with the facilitated transfer of Ag^+. From the anodic stripping voltammetry of silver on 25-μm Pt microdisk electrode, no differences were observed between the cases with and without 500 μM 4-AP at pH values of 6.4 and 9.4 respectively (data not shown). These results indicate that the micropipet-supported ITIES tip is suitable for measuring the concentration of Ag^+ in the presence of Mg^{2+}, Na^+, K^+, and 4-AP cations. Fig. 1 *Inset* shows a differential pulse voltammogram (DPV) of the facilitated Ag^+ transfer by silver ionophore IV, which provides an alternative method of measuring the Ag^+ concentration. Because the micropipette could only be used once, every micropipette used for a group of experiments was calibrated with a standard aqueous solution of 100 μM Ag_2SO_4. In this article, all of the Ag^+ concentrations were calculated from the results from DPV because the peak current response of DPV could be determined more conveniently and precisely, especially with low silver concentrations.

Effect of 4-AP on Silver Uptake by Fibroblasts. Silver-containing antimicrobial drugs are often used on the skin, for example, in the treatment of burns, so the effect of Ag^+ ion on mammalian fibroblasts is of interest. In another study (D.Z., X. Li, A. B. Nepomnyashchii, M. A. Aviles, F.-R.F.F., and A. J. Bard, unpublished work), viability of fibroblasts, determined by their respiration, was a function of the Ag^+ concentration. After Ag^+ was taken up by the fibroblasts, it was reduced to form metallic silver in cells held on SECM stage overnight. We also reported our methodology of monitoring Ag^+ uptake by the fibroblasts with time by using the Ag^+-ISE as an SECM tip (30). Because Ag^+ is not an essential cation for organisms and is not hydrophobic enough to penetrate the cell membrane directly, Ag^+ could employ other cation channels, for example, Na^+ ion channels (34) or the Cu^{2+} transport system (10, 11). Because the physical properties of K^+ (Pauling radius, 1.33 Å; diffusion coefficient, D, 1.96 $\times$ 10^{-5} cm^2/s) and Ag^+ (1.26 Å; D, 1.65 $\times$ 10^{-5} cm^2/s) are similar (35, 36), the K_v channels are interesting possibilities.

Fig. 2 *Inset* shows a schematic diagram of the set-up used for monitoring Ag^+ uptake by a monolayer of fibroblast cells. The Ag^+-ISE was positioned $\approx$1 mm above the cells, which is far enough to show the concentration change in the bulk of the drop. After the sulfate medium drop was replaced by a 100-μl drop of sulfate medium containing 100 μM Ag_2SO_4, the change of Ag^+ concentration with time was recorded immediately, and then as a function of time, by DPV. The Ag^+ concentrations in the drop at different times after the Ag^+-containing sulfate medium was applied to the fibroblasts in the presence or absence of 0.2 mM 4-AP is shown in Fig. 2. Note that the amount of Ag^+ taken up by the fibroblasts in the presence of 4-AP was significantly larger than the case in which 4-AP was absent. The rate of Ag^+ uptake with 4-AP was also faster because the time when steady state was achieved was shortened.

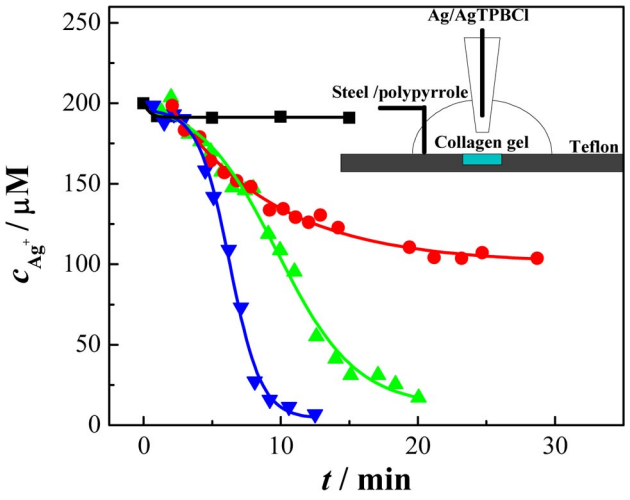

Fig. 3. Ag^+ concentration changes with time when *E. coli* implanted collagen gel exposed to: (*i*) 0.1 mM Ag_2SO_4, collagen gel without *E. coli* (black squares); with *E. coli*: (*ii*) 0.1 mM Ag_2SO_4 (red circles), (*iii*) 0.1 mM Ag_2SO_4 and 0.5 mM 4-AP (green triangles), and (*iv*) 0.1 mM Ag_2SO_4 and 1 mM 4-AP (blue inverted triangles). (Inset) Schematic diagram for detection of Ag^+ concentration in the bulk drop.

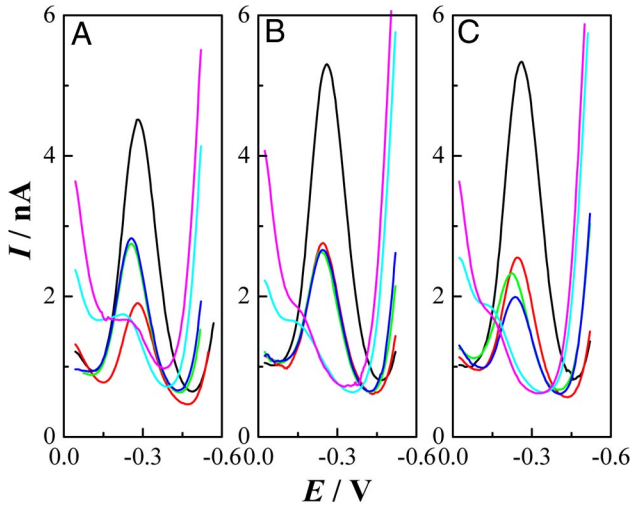

Fig. 4. Differential pulse voltammograms of Ag^+ concentration after *E. coli* suspended in different sulfate culture mediums for different time: (*A*) 2 min; (*B*) 5 min, and (*C*) 10 min. Black line, calibrate DPVs of 0.1 mM Ag_2SO_4 only; red line, *E. coli* exposure to 0.1 mM Ag_2SO_4; green line, *E. coli* exposure to 0.1 mM Ag_2SO_4 + 0.1 mM 4-AP; blue line, *E. coli* exposure to 0.1 mM Ag_2SO_4 + 0.2 mM 4-AP; cyan line, *E. coli* exposure to 0.1 mM Ag_2SO_4 + 0.5 mM 4-AP; and magenta line, *E. coli* exposure to 0.1 mM Ag_2SO_4 + 1 mM 4-AP.

Effect of 4-AP on Silver Uptake by *E. coli*. We also examined Ag^+ uptake in *E. coli*, a model used frequently for the evaluation of antimicrobial drugs. Because *E. coli* cells do not attach spontaneously to the bottom of the Petri dish, collagen type I was used to immobilize *E. coli* following the procedure reported elsewhere (37). Fig. 3 *Inset* shows the schematic diagram for monitoring the Ag^+ uptake by *E. coli* cells immobilized in a 3D collagen type I gel. Same as in the fibroblast studies, the Ag^+ concentration change in the bulk solution was monitored with time by DPV. Fig. 3 shows typical Ag^+ uptake by *E. coli* for different cases. Because the collagen gel is a hydrogel, silver ions can readily diffuse into it, as shown in curve 1 in the absence of *E. coli*, where a steady state is attained after ≈2 min with only a slight decrease in the Ag^+ concentration. Curve 2 shows the case of *E. coli*-collagen exposure to 100 μM Ag^+, whereas curves 3 and 4 show Ag^+ with two different concentrations of 4-AP. When the concentration of 4-AP was 0.5 mM, the amount of Ag^+ taken up by *E. coli* was significantly promoted and the time taken to reach steady state decreased. These results are similar to the case of mammalian fibroblasts.

To elucidate the validity of these results, experiments were also done with the *E. coli* suspensions. The *E. coli* cells were harvested through centrifugation and washed with sterile distilled water several times to remove the residual anions adhering to the outside surface of the cells. Then, *E. coli* cells were exposed to the Ag^+-containing sulfate medium with different concentrations of 4-AP and DPVs were taken as a function of time. As shown in Fig. 4, the *E. coli* cells suspended in solutions took up Ag^+ much faster in the presence of 0.5 mM and 1 mM 4-AP. In the presence of 0.1 mM and 0.2 mM 4-AP, in the first 2 min, the relative amount of Ag^+ taken up was lower than that in the absence of 4-AP. Five minutes later, it reached nearly the same value. After 10 min, the amounts were slightly more than the latter. A dose that increases the uptake was estimated to be approximately ≥0.5 mM.

Another check on the silver uptake was the measurement of the respiration, and thus viability, of *E. coli* cells in the collagen gel. Because Ag^+ could be reduced to metallic silver, which might give a positive feedback for regular redox mediators such as ferrocenemethanol in our previous study, here we used a mercury hemisphere ultramicroelectrode as the SECM tip to monitor oxygen concentration above the living cells. The more active the cells were, the greater the oxygen consumed and, consequently, the lower the SECM tip current for oxygen reduction in the vicinity of the cells. In these experiments, 10 μl of *E. coli* implanted collagen was injected into a Teflon well with a diameter of 2 mm and a depth of 1 mm. Fig. 5 shows the lateral probe scanning results of cell viability in different cases. Fig. 5 *Inset* is a schematic diagram of a lateral probe scanning experimental arrangement. The tip was scanned across the interface between the Teflon and the collagen-containing well. In a

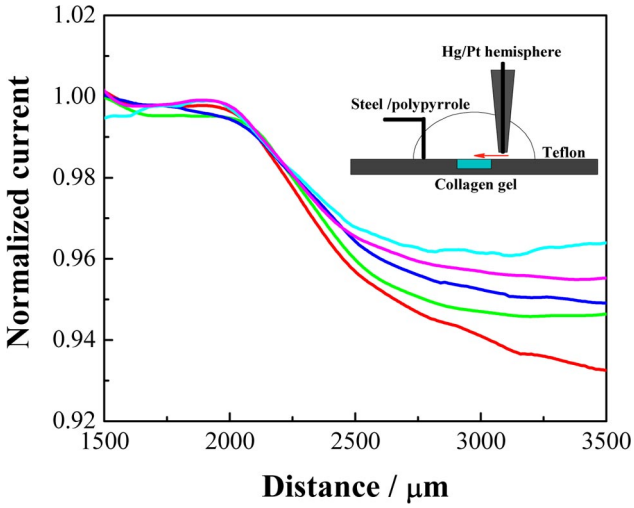

Fig. 5. SECM lateral probe scanning curves for oxygen reduction by using a mercury hemispheric electrode. The tip scanned from the Teflon substrate through the *E. coli* implanted collagen gel region after 10 min of exposure to sulfate medium: (*i*) red line, without Ag^+; (*ii*) green line, with 0.2 mM Ag^+; (*iii*) blue line, with 0.2 mM Ag^+ and 0.5 mM 4-AP; (*iv*) magenta line, with 0.2 mM Ag^+ and 1.0 mM 4-AP; (*v*) cyan line: no *E. coli* cells implanted. Because the cells consume oxygen, the tip currents above the cell region are lower than the Teflon region. The controlled one (cyan) shows the spatial effect of the slightly convex collagen gel.

control without cells, the current decreased over the collagen because it extended slightly above the Teflon level, so diffusion of oxygen to the tip was partially blocked (as usual in negative feedback SECM above insulators). The uptake of oxygen was greatest over the cells that were not treated with Ag^+. The respiration rate (uptake of oxygen) by the *E. coli* cells in the presence of Ag^+ and 4-AP was consistent with the lower viability with addition of 4-AP.

Discussion

The methodologies on how a micropipet-supported Ag^+-selective ITIES tip could be used to monitor the Ag^+ uptake by fibroblasts and how Ag^+ would affect the viability of fibroblasts have been elucidated in detail elsewhere (30, 36). We extended this earlier work here to a study of the relationship between Ag^+ uptake and K_v channels. We observed that fibroblasts take up a larger amount of Ag^+, more quickly, when 4-AP was present in solution. Because 4-AP is known to interact with K_v channels, it is reasonable to attribute the increasing amount of Ag^+ ions taken up by fibroblasts to 4-AP modification of the K_v channels. The fibroblast cell density was determined by a hemocytometer before experiment and the drop volume was controlled, so the number of cells was known. From the data shown in Fig. 2, the Ag^+ uptake and the time required under different conditions could be determined. Thus, the rate of Ag^+ taken up by the fibroblasts is 4.8×10^7 ions per cell per sec in the absence of 4-AP. In the presence of 0.2 mM 4-AP in the Ag^+-containing sulfate medium, the rate of Ag^+ uptake was approximately twice as large, whereas the maximum amount of silver in the cells was also larger (8.6×10^{10} per cell without 4-AP vs. 1.2×10^{11} per cell with 0.2 mM 4-AP).

Bcause one CFU is derived from a single viable *E. coli* cell, the number of *E. coli* cells could be determined and the rate of Ag^+ uptake per cell also quantified. To determine how much Ag^+ was taken up by *E. coli*, a 3D structured hydrogel was prepared with collagen type I. As shown in Fig. 4, the *E. coli* cells suspended in the aqueous solution quickly take up Ag^+. When the 4-AP concentration was <0.5 mM, the blockage of the K_v channels did not reach the threshold point for increased Ag^+ uptake. Initially the Ag^+ uptake rate was less than the control level (i.e., with no 4-AP). It then required 5 min to reach the control level. When 4-AP was at 0.5 mM or higher, Ag^+ uptake reached saturation in 2 min. The results suggest a significant contribution of 4-AP binding to the K_v channels to this process. However, the rate of Ag^+ uptake by *E. coli* was decreased by the 3D collagen gel. From the data in Fig. 3, the uptake rates of Ag^+ by the *E. coli* cells implanted in the 3D collagen gel are 1.5×10^4, 3.5×10^4, and 5.9×10^4 ions per cell per sec for 0.1 mM Ag_2SO_4, with 0, 0.5, and 1 mM 4-AP, respectively. Because the halide concentrations were controlled, the precipitation of Ag^+ was avoided. Ag^+ ions diffused into the gel gradually where the cells took them up. When 4-AP was absent from the sulfate medium, the cells took up Ag^+ until a steady state was established. When the K_v channels were bound by 4-AP to the threshold point, the conformation of 4-AP binding K_v channel changed and another pathway of Ag^+ introduction into the cell was opened. As a result, the *E. coli* cells would continue to take up Ag^+ until a new steady state value was achieved. From Fig. 5, the respiration rate of the *E. coli* cells also decreased with an increase in the 4-AP concentration. The results show that the more Ag^+ taken up, the smaller the respiration rate of the cells, in agreement with our previous study.

K^+ channels control the electric potential across the cell membrane by allowing the rapid, selective diffusion of K^+ ions down a gradient of electrochemical potential. The structure of the K^+ channel has been reported and a K^+ transport mechanism has been proposed (38–40). How the interaction of 4-AP affects the transport of Ag^+, either through the channel itself or via the effect of field on other channels will require further study.

Conclusions

4-AP, a well known K_v channel blocker, was found to enhance the rate of Ag^+ uptake by fibroblasts and *E. coli*. When 4-AP was added with Ag^+, both the uptake rate and the total amount taken up is increased. For fibroblasts, the uptake rate is 4.8×10^7 ions per cell per sec without 4-AP compared with 1.0×10^8 ions per cell per sec with 0.2 mM 4-AP. For *E. coli* cells, the uptake rate is 1.5×10^4 ions per cell per sec without 4-AP vs. 3.5×10^4 ions per cell per sec with 0.5 mM 4-AP, and 5.9×10^4 ions per cell per sec with 1 mM 4-AP. This effect could be important in designing systems of Ag-based antibiotics.

Experimental Section

Chemicals and Materials. Calixarene-based silver ionophore IV and potassium tetrakis(4-chlorophenyl)borate were purchased from Fluka. Ag_2SO_4, bis(triphenylphosphoranylidene)ammonium chloride, and octyltriethoxysilane were supplied by Aldrich. BTPPATPBCl was prepared by the same method as reported elsewhere (41). Na_2SO_4, K_2SO_4, $MgSO_4$, NaOH, NaH_2PO_4, Na_2HPO_4, Hepes, D-glucose and DCE were obtained from Fisher. All chemicals were reagent grade and used as received. All aqueous solutions were prepared with Milli-Q deionized water (Millipore Corp.). The organic solution was prepared from purified DCE.

Dulbecco's modified Eagle's medium with L-glutamine (DMEM), FBS, dimethyl sulfoxide, and trypan blue were obtained from American Type Culture Collection, and Hepes-buffered saline solution and trypsin-neutralizing solution from Cambrex. Trypsin-EDTA solution was provided from MP Biomedicals. Miller LB broth and Lennox LB agar were purchased from Fisher. Collagen type I was purchased from BD Biosciences. All of these were used as received.

Cell Culture and Preparation. 3T3 MEFs WT fibroblast cells (CRL-275, *Mus musculus* from mouse embryo) were provided by ATCC. The fibroblasts were grown and maintained in DMEM with 10% heat-inactivated FBS while they adhered to the bottom of the Petri dish. The temperature was maintained at 37.5°C in a water-jacketed incubator (model 2310, VWR Scientific) with 5% CO_2. As reported (30), a sulfate medium was used for SECM experiments: 75 mM Na_2SO_4, 1 mM $MgSO_4$, and 3 mM K_2SO_4. The pH value was adjusted with 0.1 M NaOH to 6.5 to avoid precipitation of Ag^+. The maximum Ag^+ concentration in this medium could be calculated to be up to 17.6 mM. The procedures of cell culture, cell density evaluation, and viability determination were performed according to the instructions provided by ATCC. All of the cell sample preparations were carried out in a sterile fume hood (Liberty Co.). A 100-μl sample of the complete culture medium with a cell density of $\approx 1 \times 10^6$/ml was deposited on the bottom of a Petri dish. In general, it took 6–8 h for the fibroblasts to adhere to the bottom and form a monolayer with a coverage >90% in this medium. The fibroblasts were rinsed carefully with sterile distilled water and then with the sulfate medium, several times, to remove the residual halides and other anions on the cells to avoid precipitation of Ag^+. The cells were then covered by 100 μl of sulfate medium. After the micropipet-supported Ag^+-ISE was calibrated with a standard sulfate medium containing 100 μM Ag_2SO_4, it was removed into the sulfate medium drop covering the fibroblasts. Then, the covering medium was replaced by the one containing Ag^+ and/or 4-Ap for EC and SECM measurements.

E. coli (ATCC no. 25922) was obtained as lyophilized pellets from MicroBioLogics and grown on minimal agar plates (37°C for 48 h) by using standard bacterial culture techniques. Cells taken from the plate were then grown aerobically in broth. All stock solutions were autoclaved before use. Growth broth was vigorously stirred to ensure aeration, and cells were grown for 18 h at room temperature, until at the stationary phase. Cells were harvested by centrifugation at 8,000 rpm (VWR model Galaxy 16D) for 3 min and washed several times in preautoclaved Milli-Q water. The collected cells were suspended in preautoclaved Milli-Q water. This procedure was followed to ensure a solution free of chloride, because most of the experiments were carried out in the presence of Ag^+. The number of cells was determined by counting the colonies by a series of continued dilutions of the cell suspension that were dropped on an agar plate and cultured overnight. The initial concentration of *E. coli* cells was controlled to be $\approx 10^{11}$ colony forming units (CFU)/ml for the fabrication of collagen gels.

Because *E. coli* cells are not spontaneously attached to the bottom of a Petri dish, collagen type I was used to immobilize them. The collagen, phosphate buffer solution (250 mM NaH_2PO_4, 250 mM Na_2HPO_4), and the cell suspension

were mixed in a volume ratio of 8:1:1. Fifty microliters of *E. coli* implanted collagen was cast in a Teflon well (with a diameter of 4.2 mm and a depth of 0.6 mm.) and incubated in sterile hood at 37°C for 30 min to form a flat gel plane. After rinsing several times with the sulfate medium to remove the phosphate ions, the sample was fixed on the SECM stage for EC and SECM experiments. To elucidate the enhancement of Ag^+ uptake by 4-AP, 200-μl *E. coli* suspensions were mixed with 200 μl of sulfate medium containing different concentrations of Ag^+ and 4-AP for 2, 5, and 10 min, respectively, and then centrifuged. The clear solution was separated and the residual Ag^+ was detected by the amperometric Ag^+-ISE.

Instruments. An Olympus inverted microscope (Olympus Co.) was used to observe the cell coverage and growth status of the fibroblast cells. Micropipets were prepared with a model-2000 laser puller (Sutter Instrument Co.) as described elsewhere (42). The Olympus microscope was used to examine the quality and measure the diameter of the micropipet. Ag wire with a diameter of 100 μm was anodized in DCE solution with 5 mM BTPPATPBCl overnight to form a layer of AgTPBCl. The AgTPBCl-coated Ag wire was inserted into a micropipet as the reference electrode in the DCE phase. To avoid Ag^+ contamination, polypyrrole-coated stainless steel was used as reference electrode in the aqueous solution (43). All of the EC measurements were performed with a commercial SECM workstation (CH Instrument Co.).

ACKNOWLEDGMENTS. D.Z. thanks Dr. Jie Luo (Department of Human Ecology, University of Texas at Austin) and Dr. Shanqing Gu (Institute for Cellular and Molecular Biology, University of Texas at Austin) for their help with bacterial culture and characterization. This work was supported by NUCRYST Pharmaceuticals.

1. Russell AD, Hugo WB (1994) Antimicrobial activity and action of silver. *Prog Med Chem* 31:351–370.
2. Grier N (1977) *Disinfection, Sterilization and Preservation*, ed Block SS (Lea and Febiger, Philadelphia), pp 295–407.
3. Rogers KS (1972) Variable sulfhydryl activity toward silver nitrate by reduced glutathione and alcohol, glutamate and lactate dehydrogenase. *Biochim Biophys Acta* 263:309–314.
4. Yudkin J (1941) The effect of silver ions on some enzymes of bacterium coli. *Enzymologia* 2:161–170.
5. Bragg PD, Rainnie DJ (1974) The effect of silver ions on the respiratory chain of Escherichia coli. *Can J Microbiol* 20:883–889.
6. Kostyrko VA, *et al.* (1991) The H^+-motive ans Na^+-motive respiratory chains in Bacillus FTU subcellular vesicles. *Eur J Biochem* 198:527–534.
7. Semeykina AL, Skulachev VP (1990) Submicromolar Ag^+ increase passive Na^+ permeability and inhibits the respiration-supported formation of Na^+ gradient in *Bacillus* FTU vesicles. *FEBS Lett* 269:69–72.
8. Dibrov P, Dzioba J, Gosink KK, Häse CC (2002) Chemiosmotic mechanism of antimicrobial activity of Ag^+ in Vibrio cholerae. *Antimicrob Agents Chemother* 46:2668–2670.
9. Schreurs WJA, Rosenberg H (1982) Effect of silver on transport and retention of phosphate by *Escherichia coli*. *J Bacteriol* 152:7–13.
10. Solioz M, Odermatt A (1995) Copper and silver transport by CopB-Atpase in membrane vesicles of *Enterococcus hirae*. *J Biol Chem* 270:9217–9221.
11. Ghandour W, Hubbard JA, Deistung J, Hughes MN, Poole RK (1998) The uptake of silver ion by *Escherichia coli* K12: Toxic effect and interaction with copper ions. *Appl Microbiol Biotechnol* 28:559–565.
12. Hughes MN, Poole PK (1989) *Metals and Microorganisms* (Chapman and Hall, London) pp 287–291.
13. Slawson RW, Van Dyke MI, Trevors JT (1992) *Accumulation and Toxicity in Microorganisms* (Academic/Elsevier, Philadelphia).
14. Poon VKM, Burd A (2004) *In vivo* cytotoxicity of silver: Implication for clinical wound care. *Burns* 30:140–147.
15. Hidalgo E, Dominguez C (1998) Study of cytotoxicity mechanisms of silver nitrate in human dermal fibroblasts. *Toxicol Lett* 98:169–179.
16. Deshpande LM, Chopade RA (1994) Plasmid mediate silver resistance in *Acinitobacter baumannii. Biometals* 7:49–56.
17. Henry AT, Stewart IO (1979) Silver-resistant *Enterobacteriaceae* from hospital patients. *Can J Microbial* 25:915–921.
18. Silver S, Phung LT (1996) Bacterial heavy metal resistance mechanism: New surprise. *Annu Rev Microbiol* 50:753–789.
19. Nikaido H (1994) Prevention of drug access to bacterial targets: Role of permeability barrier and active efflux. *Science* 264:382–388.
20. Silver S (2003) Bacterial silver resistance: Molecular biology and uses and misuses of silver compounds. *FEMS Microbiol Rev* 27:341–353, and references therein.
21. Judge SIV, Jr, Bever CT (2006) Potassium channel blockers in multiple sclerosis: Neuronal Kv Channels and effects of symptomatic treatment. *Pharmacol Ther* 111:224–259.
22. Mathie A, Wooltorton JRA, Watkins CS (1998) Voltage-activated potassium channels in mammalian neurons and their block by novel pharmacological agents. *Gen Pharm* 30:13–24.
23. Howe JR, Ritchie JM (1991) On the active form of 4-aminopyridine: Block of K^+ currents in rabbit schwann cells. *J Physiol* 433:183–205.
24. Choquet D, Korn H (1992) Mechanism of 4-aminopyridine action on voltage-gated potassium channels in lymphocytes. *J Gen Physiol* 99:217–240.
25. Bard AJ, Mirkin MV, eds (2001) *Scanning Electrochemical Microscopy* (Marcel Dekker, New York), pp 445–512.
26. Bard AJ, Li X, Zhan W (2006) Chemically imaging living cells by scanning electrochemical microscopy. *Biosens Bioelectron* 22:461–472.
27. Amemiya S, Guo J, Xiong H, Gross DA (2006) Biological applications of scanning electrochemical microscopy: Chemical imaging of single living cells and beyond. *Anal Bioanal Chem* 386:458–471.
28. Mauzeroll J, Bard AJ, Owhadian O, Monks TJ (2004) Menadione metabolism to thiodione in hepatoblastoma by scanning electrochemical microscopy. *Proc Natl Acad Sci USA* 101:17582–17587.
29. Mauzeroll J, Bard AJ (2004) Scanning electrochemical microscopy of menadione-glutathione conjugate export from yeast cells. *Proc Natl Acad Sci USA* 101:7862–7867.
30. Zhan D, Li X, Zhan W, Fan FF, Bard AJ (2007) Scanning Electrochemical Microscopy 58. The application of a micropipette-supported ITIES Tip to detect Ag^+ and study its effect on fibroblast cells. *Anal Chem* 79:5225–5231.
31. Merroun ML, Omar NB, Alonso E, Arias JM, Gonzalez-Munoz MT (2001) Silver sorption to *Myxococcus xanthus. Geomicrobiol J* 18:183–193.
32. Samec Z (2004) Electrochemistry at the interface between two immiscible electrolyte solutions. *Pure Appl Chem* 76:2147–2180.
33. Samec Z, Samcová E, Girault HH (2004) Ion amperometry at the interface between two immiscible electrolyte solutions in view of realizing the amperometric ion-selective electrode. *Talanta* 63:21–32.
34. Bury NR, Wood CM (1999) Mechanism of branchial apical silver uptake by rainbow trout is via the proton-coupled Na^+ channel. *Am J Physiol Regulatory Integrative Comp Physiol* 277:1385–1391.
35. Marcus Y, ed (1997) *Ion Properties* (Dekker, New York).
36. Camino D, Yellen G (2001) Tight steric closure at the intracellular activation gate of a voltage-gated K^+ channel. *Neuron* 32:649–656.
37. Kaya T, *et al.* (2004) Respiration activity of Escherichia coli entrapped in a cone-shaped microwell and cylindrical micropore monitored by scanning electrochemical microscopy (SECM). *Analyst* 129:529–534.
38. Doyle DA, *et al.* (1998) The structure of the potassium channel: Molecular basis of K+ conduction and selectivity. *Science* 280:69–77.
39. Zhou Y, Morais-Cabral JH, Kaufman A, MacKinnon R (2001) Chemistry of ion coordination and hydration revealed by a k^+ channel-fab complex at 2.0Å resolution. *Nature* 414:43–48.
40. Zhou Y, MacKinnon R (2003) The occupancy of ions in the K^+ selectivity filter: Charge balance and coupling of ion binding to protein conformational change underlie high conduction rates. *J Mol Biol* 333:965–975.
41. Lee HJ, Beriet C, Girault HH (2002) Amperometric detection of alkali metal ions on micro-fabricated composite polymer membranes. *J Electroanal Chem* 453:211–219.
42. Zhan D, *et al.* (2004) Electrochemical investigation of dopamine at the water/1,2-dichloroethane interface. *Anal Chem* 76:4128–4136.
43. Ghilane J, Hapiot P, Bard AJ (2001) Metal/polypyrrole quasi-reference electrode for voltammetry in nonaqueous and aqueous solutions. *Anal Chem* 78:6868–6872.